Effect of anisotropic collisions on solar scattering polarization

Saleh Qutub[1], Moncef Derouich[1,2] and Badruddin Zaheer Ahmad[1]

[1] Astronomy and Space Science Department, Faculty of Science, King Abdulaziz University, Jeddah 21589, Saudi Arabia; *squtub@kau.edu.sa*

[2] Sousse University, ESSTHS, Lamine Abbassi Street, 4011 H. Sousse, Tunisia

Abstract Scattering of anisotropic radiation by atoms, ions or molecules is sufficient to generate linear polarization observable in stars' and planets' atmospheres, circumstellar environments, and in particular in the Sun's atmosphere. This kind of polarization is called scattering polarization (SP) or second solar spectrum (SSS) if it is formed near the limb of the solar photosphere. Generation of linear SP can typically be reached more easily than circular SP. Interestingly, the latter is often absent in observations and theories. Intrigued by this, we propose to demonstrate how circular SP can be created by anisotropic collisions if a magnetic field is present. We also demonstrate how anisotropic collisions can result in the creation of circular SP if the radiation field is anisotropic. We show that under certain conditions, linear SP creation is accompanied by the emergence of circular SP which can be useful for diagnostics of solar and astrophysical plasmas. We treat an example and calculate the density matrix elements of tensorial order $k = 1$ which are directly associated with the presence of circular SP. This work should encourage theoretical and observational research to be increasingly oriented towards circular SP profiles in addition to linear SP in order to improve our analysis tools of astrophysical and solar observations.

Key words: Scattering processes — Line: formation - Polarization — Sun: magnetic fields

1 STATEMENT OF THE PROBLEM

Symmetry-breaking processes, such as (de-)excitations by anisotropic light or anisotropic collisions, could generate the so-called scattering polarization (SP) of the emitted light. An atom is said to be polarized by scattering if the scattering processes result in an uneven population of its Zeeman sublevels and thereby the appearance of coherences between them. This is what is referred to as atomic polarization (e.g., Sahal-Brechot 1977; Trujillo Bueno 2001; sect. 3.6 of Landi Degl'Innocenti & Landolfi 2004). For an in-depth understanding of astrophysical/solar plasma, the polarization properties of light emitted by atoms/ions/molecules must be carefully studied from observational and theoretical points of view. In this context, newer theoretical techniques and modern instruments allowing observation and interpretation of small polarization signals are needed.

The effect of collisions on atomic states $|\alpha J\rangle$, and therefore on the SP, can be described by the polarization transfer and relaxation rates; here J denotes the total angular momentum and α represents the other quantum numbers associated with the atomic state. For the study

of polarization of spectral lines it is more convenient to use the density matrix formalism expressed in the basis of irreducible tensorial operators, T_q^k. In this framework, the density matrix elements $\rho_q^k(\alpha J)$ give the average state of the polarized atom which emits the polarized light (see e.g., sects. 3.6 and 3.7 of Landi Degl'Innocenti & Landolfi 2004). Here k is the tensorial order and q is the coherence between the Zeeman sublevels, where $0 \leq k \leq 2J$ and $-k \leq q \leq k$. The element $\rho_{q=0}^{k=0}(\alpha J)$ is related to the population of the J-level whereas elements with $k \geq 1$ characterize the polarization state of the atom and consequently of the emitted radiation. In particular, the circular SP represents the observational signature of the *orientation* of atomic levels and is quantified by the density matrix elements with odd rank, $\rho_q^{k=1}(\alpha J)$, $\rho_q^{k=3}(\alpha J)$, etc., while linear SP is associated with the atomic level *alignment* which is characterized by even tensorial order density matrix elements, $\rho_q^{k=2}(\alpha J)$, $\rho_q^{k=4}(\alpha J)$, etc.

In the solar context, observations with the THÉMIS telescope (Spain) and with the Advanced Solar Polarimeter (USA) by López Ariste et al. (2005) have revealed the existence of unexpected circular SP (symmetric V-Stokes)

of the Hα line which cannot be attributed to the Zeeman effect. On the contrary, by using the ZIMPOL telescope, Ramelli et al. (2005) observed V profiles showing an antisymmetric shape typically due to the Zeeman effect. Let us recall that symmetric V-Stokes profiles are related to circular SP and hence to the orientation of the atomic level (i.e., $\rho_q^k(\alpha J)$ with odd k), while anti-symmetric V-Stokes are known to be due to the Zeeman effect. In light of these contradictory observations, theoretical interpretation seems to be necessary. Roberto Casini & Manso Sainz (2006) proposed that the observation of symmetric V-Stokes could be due to the effect of an electric field. Derouich (2007) proposed a scenario based on impact circular polarization by anisotropic collisions. In addition, linear-to-circular SP transfer processes have been highlighted theoretically by Manabe et al. (1979) and measured experimentally by the same authors in 1981 (Manabe et al. 1981). Similar processes have been reported also by Petrashen' et al. (1993), which also contains extensive references.

It is well known that isotropic collisions can only result in the decrease of atomic polarization (e.g., Derouich et al. 2003). However, anisotropic collisions can create or increase the polarization of $|\alpha J\rangle$ levels. The variation of the atomic polarization may be due to transitions between Zeeman sublevels of the same electronic level $|\alpha J\rangle$ and/or between two different electronic levels. This can roughly be interpreted as the transfer of anisotropy from the relative velocity distribution of the colliding partners to the population of the Zeeman sublevels of the electronic sublevels involved in the transitions (e.g., D'yakonov & Perel 1978).

Now consider an ensemble of atoms illuminated by unpolarized light having cylindrical symmetry around an axis $z_{\rm rad}$. The atoms also undergo anisotropic collisions with beams of perturbers having axial symmetry around an axis $z_{\rm pert}$. Furthermore, in a magnetized plasma like the Sun, the Hanle effect of a magnetic field is an important ingredient in modeling the polarization state (e.g., Hanle 1924, sect. 10.3 of Landi Degl'Innocenti & Landolfi 2004; Derouich et al. 2007; del pino Alemán 2018). Let us therefore consider a general case of a magnetic field oriented along an axis $z_{\rm mag}$ which is neither parallel to $z_{\rm rad}$ nor parallel to $z_{\rm pert}$. The geometrical configuration of the different axes is depicted in Figure 1. Our aim in this work is to demonstrate that, under these conditions, mixing between even and odd tensorial orders is allowed and can be highlighted theoretically and observationally by obtaining non-zero circular SP (i.e., symmetric V-Stokes signals).
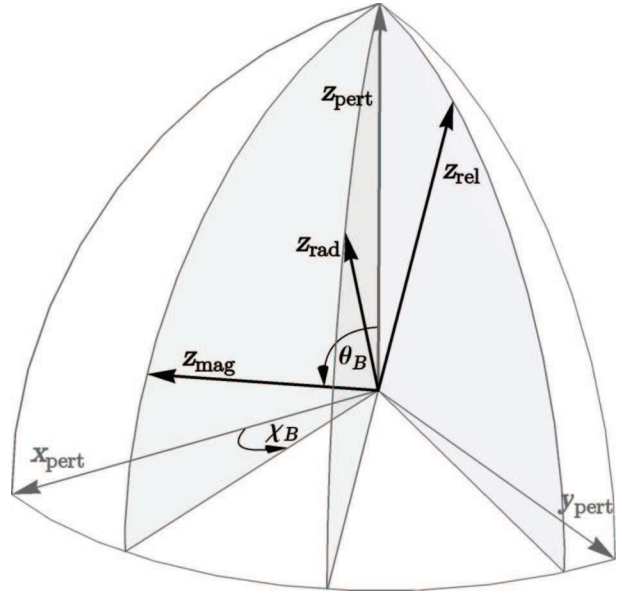

Fig. 1 Geometrical configuration of the different axes drawn in the reference frame Σ. For a given binary collision, the relative velocity of the colliding partners, $v_{\rm rel}$, points in the direction of the emitter-perturber axis, $z_{\rm rel}$.

2 THEORETICAL CONSIDERATIONS

In order to solve the statistical equilibrium equations (SEE) for the atomic levels $|\alpha_i J_{\alpha_i}\rangle$ of the emitting atom described by the elements $\rho_q^k(\alpha_i J_{\alpha_i})$, we place ourselves in a reference frame, Σ, centered on the atom and having its z-axis in the $z_{\rm pert}$ direction. The frame Σ is obtained by a rotation $\mathrm{R_B} \equiv \mathrm{R}(\text{-}\gamma_{\rm B}, \text{-}\theta_{\rm B}, \text{-}\chi_{\rm B})$ of the magnetic reference defined by the $z_{\rm mag}$-axis (see Fig. 1)[1]. The collisional cross sections are usually obtained in the collision frame having its z-axis joining the perturber and the perturbed atom ($z_{\rm rel}$ in Fig. 1), and then rotated to the frame Σ where the average over relative velocity distribution is performed. In fact in the latter frame, the symmetry properties of the collisional rates are manifest which simplifies the solution of SEE. The radiative contributions to the SEE are also rotated to the frame Σ. It can be proved that the expressions for relaxation and transfer radiative rates are formally invariant under rotation (see e.g., pages 330–331 of Landi Degl'Innocenti & Landolfi 2004).

In the basis of irreducible tensorial operators and in the reference Σ, the time variation of the elements $\rho_q^k(\alpha_i J_{\alpha_i})$ can be written as (see e.g., pages 284–285 of Landi Degl'Innocenti & Landolfi 2004; Manabe et al. 1979):

---

[1] Since the magnetic kernel $\mathcal{K}_{qq'}^k(\mathrm{R_B})$ is independent of the Euler angle $\gamma_{\rm B}$, it can be arbitrarily set to zero, $\gamma_{\rm B} = 0$ (see e.g., page 548 of Landi Degl'Innocenti & Landolfi 2004).

$$\frac{d}{dt}\rho_q^k(\alpha_i J_{\alpha_i}) = -i\omega_{L,\alpha_i J_{\alpha_i}} g_{\alpha_i J_{\alpha_i}} \sum_{q'} \mathcal{K}_{qq'}^k(R_B)\rho_{q'}^k(\alpha_i J_{\alpha_i})$$

$$- \sum_{k'q'} \left[r_A(\alpha_i J_{\alpha_i} kqk'q') + r_E(\alpha_i J_{\alpha_i} kqk'q') \right]$$

$$\rho_{q'}^{k'}(\alpha_i J_{\alpha_i})$$

$$+ \sum_{\substack{jk'q'\\j<i}} t_A(\alpha_i J_{\alpha_i} kq, \alpha_j J_{\alpha_j} k'q')\rho_{q'}^{k'}(\alpha_j J_{\alpha_j})$$

$$+ \sum_{\substack{jk'q'\\j>i}} t_E(\alpha_i J_{\alpha_i} kq, \alpha_j J_{\alpha_j} k'q')\rho_{q'}^{k'}(\alpha_j J_{\alpha_j})$$

$$+ \sum_{jk'q'} \mathcal{T}_{qq'}^{kk'}(\alpha_i J_{\alpha_i} \leftarrow \alpha_j J_{\alpha_j})\rho_{q'}^{k'}(\alpha_j J_{\alpha_j})$$

$$- \sum_{jk'q'} \mathcal{R}_{qq'}^{kk'}(\alpha_i J_{\alpha_i} \rightarrow \alpha_j J_{\alpha_j})\rho_{q'}^{k'}(\alpha_i J_{\alpha_i}).$$

$$(1)$$

For simplicity, we have ignored stimulated emissions since they are negligible in natural plasma such as the solar atmosphere. The term $-i\omega_{L,\alpha_i J_{\alpha_i}} g_{\alpha_i J_{\alpha_i}} \sum_{q'}\mathcal{K}_{qq'}^k(R_B)\rho_q^k(\alpha_i J_{\alpha_i})$ corresponds to the Hanle effect of magnetic field in the Σ reference, where $\omega_{L,\alpha_i J_{\alpha_i}} = 2\pi\nu_{L,\alpha_i J_{\alpha_i}}$ denotes the Larmor angular frequency and $g_{\alpha_i J_{\alpha_i}}$ signifies the Landé g-factor. The expression for the magnetic kernel $\mathcal{K}_{qq'}^k(R_B)$ can be found, for example, on page 548 of Landi Degl'Innocenti & Landolfi (2004). r_E and r_A respectively denote the relaxation rates due to spontaneous emission and absorption, while t_E and t_A respectively signify the transfer rates due to spontaneous emission and absorption. Expressions for these radiative rates can be found in the literature (see e.g., Bommier & Sahal-Brechot 1978, pages 287–288 of Landi Degl'Innocenti & Landolfi 2004).

We note here that due to mixing under rotation, the coherences in the radiation field tensor, $J_{q_r}^{k_r}$ responsible for the radiative rates r_A and t_A, are present in the frame, Σ, despite being non-existent in the radiation frame. $\mathcal{T}_{qq'}^{kk'}(\alpha_i J_{\alpha_i} \leftarrow \alpha_j J_{\alpha_j})$ and $\mathcal{R}_{qq'}^{kk'}(\alpha_i J_{\alpha_i} \rightarrow \alpha_j J_{\alpha_j})$ denote the collisional transfer and relaxation rates, respectively. The quantity $\mathcal{T}_q^{kk'}(\alpha_i J_{\alpha_i} \leftarrow \alpha_j J_{\alpha_j})$ represents the gain due to collisional transitions from other levels ($j \neq i$) and sublevels of the same level ($j = i$) in contrast to $\mathcal{R}_q^{kk'}(\alpha_i J_{\alpha_i} \rightarrow \alpha_j J_{\alpha_j})$ which represents the relaxation (loss) due to collisional transitions to other levels ($j \neq i$) and sublevels of the same level ($j = i$). In the dyadic basis, for collisional transition taking place within the same level ($j = i$), $\mathcal{R}_q^{kk'}$ is associated with the term $\sum_{M'\neq M} \mathcal{R}_{elastic}(\alpha_j jM \rightarrow \alpha_j jM') \times \rho(\alpha_j jM)$ and $\mathcal{T}_q^{kk'}$ contains the term $\sum_{M'\neq M} \mathcal{T}_{elastic}(\alpha_J JM \leftarrow \alpha_J JM') \times \rho(\alpha_J JM')$ (see, e.g., Derouich et al. 2003). The rates $\mathcal{T}_{elastic}$ and $\mathcal{R}_{elastic}$ are not equal since they

are related to two different transitions. Therefore, the quantities $\mathcal{T}_q^{kk'}(\alpha_i J_{\alpha_i} \leftarrow \alpha_i J_{\alpha_i})$ and $\mathcal{R}_{qq'}^{kk'}(\alpha_i J_{\alpha_i} \rightarrow \alpha_i J_{\alpha_i})$ are in general different in value. It can be noticed that even if they are equal our solutions of the SEE remain valid and, as can be verified in the next section, the orientation emergence will be clearly possible. The expression for the collisional rates in the case of axial symmetry around the axis z_{pert} can be found, for example, in Derouich (2007) and Manabe et al. (1979).

Axial symmetry of collisions combined with the Hermiticity of the density matrix dictate that (e.g., Omont 1977 and Manabe et al. 1979):

$$\mathcal{T}_{qq'}^{kk'} = 0 \quad \text{for } q \neq q', \quad \text{i.e.,} \quad \mathcal{T}_{qq'}^{kk'} = \delta_{qq'}\mathcal{T}_{qq}^{kk'} = \mathcal{T}_q^{kk'},$$
$$\mathcal{T}_{-q}^{kk'} = (-1)^{k+k'}\mathcal{T}_q^{kk'},$$

$$(2)$$

and

$$\mathcal{T}_q^{kk'} = \begin{cases} \textbf{Real} & \text{for even } k+k' \\ \textbf{Imaginary} & \text{for odd } k+k' \text{ and } q \neq 0 \,. \\ \textbf{0} & \text{for odd } k+k' \text{ and } q=0 \end{cases}$$

$$(3)$$

$\mathcal{R}_{qq'}^{kk'}$ have similar properties as $\mathcal{T}_{qq'}^{kk'}$.

For simplicity, let us consider a two-level system with unpolarizable ground state $J_{\alpha_l} = 0$. Since the ground state is unpolarizable, we are interested only in atomic polarization of the excited state. Thus, our intention is to obtain ρ_q^k elements describing the state of the excited level and characterizing its atomic polarization in the reference Σ (e.g., Derouich et al. 2007). We focus on the alignment (ρ_q^k with even k)-to-orientation (ρ_q^k with odd k) transfer within the polarizable upper level. Alignment-to-orientation transfer by anisotropic collisions could explain, for instance, solar observations of circular SP by López Ariste et al. (2005). To demonstrate the possibility of circular SP creation by collisions, one must determine orientation elements $\rho_q^{k=odd}$ to confirm that they are not equal to zero. We solve the SEE, given by Equation (1), in the reference frame Σ. The Euler angles of the rotation $R(-\gamma_B, -\theta_B, -\chi_B)$ are between the magnetic reference and the frame Σ.

For the purpose of illustration, we take the total angular momentum of the excited state, J_{α_u}, to be 1. Further for simplicity, we take z_{mag} to be in the $\{xz\}_{pert}$-plane, i.e., we set the azimuthal angle $\chi_B = 0$. In what follows, we replace the notations J_{α_l} and J_{α_u} by 0 and 1, respectively. For example $\mathcal{R}_1^{11}(1,0)$ correspond to the relaxation rates $\mathcal{R}_q^{kk'}$ associated with the loss of electrons from the level $J_{\alpha_u} = 1$ to the level $J_{\alpha_l} = 0$ where $k = k' = 1$ and $q = 1$. $\mathcal{R}_1^{11}(1)$ are the relaxation rates due to elastic collisions within the same level $J_{\alpha_i} = 1$. Similarly, $\mathcal{T}_0^{20}(1,0)$ is the gain of electrons going from the level $J_{\alpha_l} = 0$ to the level $J_{\alpha_u} = 1$ where $k = 2$,

$k' = 0$ and $q = 0$ and $\mathcal{T}_0^{20}(1)$ represents the gain due to electrons transferring from sublevels within the same level. Physically, the collisional relaxation corresponds to the loss of atomic q-coherence/k-order of the level under consideration. In contrast, the transfer rates correspond to the gain of coherence or order coming from other levels and sublevels of the same level. Collisional contribution to the evolution of the density-matrix elements is due to transfer and relaxation rates. The full set of SEE describing the two-level system under consideration is provided in Appendix A. Let us mention that we used the same way to denote the density matrix elements as for collisional rates, for instance $\rho_1^1(1)$ represents the density matrix element where $k = 1$, $q = 1$ and $J_{\alpha_l} = 1$.

Solution of the SEE in the general case, where the three sources of anisotropy discussed above are all present, leads to very large expressions which we do not show here. Instead, we consider some special cases in which two sources of anistropy are present at a time. As we affirm below, this is enough to illustrate our main point; namely, the breaking of cylindrical symmetry could lead to the emergence of circular SP. In addition, we give only the $\rho_0^1(\alpha_u J_{\alpha_u})$ and $\rho_1^1(\alpha_u J_{\alpha_u}) = \mathrm{Re}\rho_1^1(\alpha_u J_{\alpha_u}) + \mathrm{i}\,\mathrm{Im}\rho_1^1(\alpha_u J_{\alpha_u})$ to demonstrate that it is possible to obtain orientation with $k = 1$ (circular polarization) from alignment with $k = 2$ (linear polarization). Other expressions of $\rho_q^k(\alpha_i J_{\alpha_i})$ can be obtained from the set of SEE in Appendix A.

3 SOLUTIONS OF THE SEE AND DISCUSSION

As discussed above, in a spherically symmetric situation, the atomic polarization, if at all present, can only decrease. Reduction in the symmetry of the problem leads to the formation or increase of SP. For example, linear SP can be created in the presence of anisotropic radiation (e.g., sect. 10.2 of Landi Degl'Innocenti & Landolfi 2004) or anisotropic collisions (e.g., Sahal-Brechot et al. 1996; Vogt et al. 2001). We now show that further reduction in the symmetry of the problem can lead to the generation of circular SP.

3.1 Anisotropic Collisions and Anisotropic Radiation Field:

We first consider the case where axially symmetric collisions and an axially symmetric unpolarized radiation field, whose axes of symmetry are in general not parallel to each other, are present. The SEE describing the situation are obtained from those in Appendix A by setting $\omega_{\mathrm{L}} = 0$. These SEE can be easily solved to obtain the density matrix. The elements of the density matrix with $k = 1$ are

defined by:

$$\rho_0^1(1) = 0\,, \tag{4}$$

$$\begin{aligned}
\rho_1^1(1) &= \mathrm{Re}\rho_1^1(1) + \mathrm{i}\,\mathrm{Im}\rho_1^1(1) \\
&= \mathscr{C}B_{01}\left(\mathrm{ImJ}_1^2 + \mathrm{i}\,\mathrm{ReJ}_1^2\right)\rho_0^0(0) \tag{5} \\
&= \mathrm{i}\,\mathscr{C}B_{01}\left(\mathrm{J}_1^2\right)^*\rho_0^0(0)\,,
\end{aligned}$$

where $\mathscr{C}$ is expressed as

$$\mathscr{C} \equiv -\frac{\mathcal{C}_1^{12}(1,0)}{\sqrt{3}\left[\left(\mathcal{C}_1^{11}(1,0) + A_{10}\right)\left(\mathcal{C}_1^{22}(1,0) + A_{10}\right) + \mathcal{C}_1^{12}(1,0)\mathcal{C}_1^{21}(1,0)\right]}\,. \tag{6}$$

Here A_{10} and B_{01} respectively denote the Einstein coefficients for spontaneous emission and photon absorption characterizing the probability of transitions between the lower level with $J_{\alpha_l} = 0$ and the upper level with $J_{\alpha_u} = 1$. We have also defined $\mathcal{C}_q^{kk'}(J_{\alpha_i}, J_{\alpha_j}) \equiv \mathcal{R}_q^{kk'}(J_{\alpha_i} \to J_{\alpha_j}) + \mathcal{R}_q^{kk'}(J_{\alpha_i} \to J_{\alpha_i}) - \mathcal{T}_q^{kk'}(J_{\alpha_i} \leftarrow J_{\alpha_i}) \equiv \mathcal{R}_q^{kk'}(J_{\alpha_i}, J_{\alpha_j}) + \mathcal{R}_q^{kk'}(J_{\alpha_i}) - \mathcal{T}_q^{kk'}(J_{\alpha_i})$ [e.g., $\mathcal{C}_1^{12}(1,0) = \mathcal{R}_1^{12}(1,0) + \mathcal{R}_1^{12}(1) - \mathcal{T}_1^{12}(1)$]. As can be seen from Equations (5) and (6), the $\rho_1^1(1)$ is non-zero, signaling the emergence of circular SP, provided that $\mathcal{C}_1^{12}(1,0)$ and $\rho_0^0(0)$ are different from zero. The rate $\mathcal{C}_1^{12}(1,0)$ is necessarily non-zero given the symmetry conditions explained in Section 2 (see e.g., Manabe et al. 1979). Further, the density matrix element of the lower level, $\rho_0^0(0)$, is expected to be different from zero since lifetime of the lower level is usually large compared to that of the upper level. This is the case even if $\mathcal{R}_q^{kk'}(J_{\alpha_i}) = \mathcal{T}_q^{kk'}(J_{\alpha_i})$ as can be verified from the definition of $\mathcal{C}_q^{kk'}(J_{\alpha_i}, J_{\alpha_j})$ above.

The generation of circular SP is clearly due to the breaking of cylindrical symmetry of the problem. Had the radiation field been isotropic or cylindrically symmetric around an axis, z_{rad}, which is parallel/anti-parallel to that of collisions, z_{pert}, there would be no coherences in the radiation field ($J_{q \neq 0}^2 = 0$ in the frame, Σ) and hence no emergence of circular SP. Similarly, if the collisions were isotropic, collisional rates with $k \neq k'$ or with $q \neq 0$ would vanish. Consequently, there would be no circular SP as can be seen from Equations (5) and (6). In the last two cases, the cylindrical symmetry of the problem is restored and thus there can only be linear SP. In other words, the generation of circular SP is possible only if the whole problem is neither isotropic nor has axial symmetry.

3.2 Anisotropic Collisions and Oriented Magnetic Field

Let us consider another case of broken axial symmetry to further illustrate our point. In this setup we have an ensemble of atoms undergoing axially symmetric collisions in the presence of an oriented magnetic field and isotropic radiation field. This case is described by the SEE

given in Appendix A while setting $J_q^2 = 0$. Solution of the SEE in this case holds:

$$\rho_0^1(1) = \frac{\sqrt{2}g_1\omega_{\mathrm{L,1}}s_{\theta_{\mathrm{B}}}\mathrm{Im}\rho_1^1(1)}{[\mathcal{C}_0^{11}(1,0) + A_{10}]}, \qquad (7)$$

$$
\begin{aligned}
\mathrm{Re}\rho_1^1(1) = \Bigg(& g_1\omega_{\mathrm{L,1}}s_{\theta_{\mathrm{B}}}\mathcal{C}_1^{12}(1,0)\Bigg\{g_1^2\omega_{\mathrm{L,1}}^2\bigg[-4g_1^2\omega_{\mathrm{L,1}}^2c_{\theta_{\mathrm{B}}}^4\big(\mathcal{C}_0^{11}(1,0)+A_{10}\big) + c_{\theta_{\mathrm{B}}}^2\Big[2g_1^2\omega_{\mathrm{L,1}}^2s_{\theta_{\mathrm{B}}}^2\big(\mathcal{C}_0^{11}(1,0)\\
& + 2\mathcal{C}_1^{22}(1,0) + 3A_{10}\big) + \big(\mathcal{C}_0^{11}(1,0)+A_{10}\big)\Big\{3A_{10}^2 + \big[4\mathcal{C}_1^{11}(1,0) + 4\mathcal{C}_1^{22}(1,0) - 2\mathcal{C}_2^{22}(1,0)\big]A_{10}\\
& - [\mathcal{C}_2^{22}(1,0)]^2 + 4\mathcal{C}_1^{12}(1,0)\mathcal{C}_1^{21}(1,0) + 4\mathcal{C}_1^{11}(1,0)\mathcal{C}_1^{22}(1,0)\Big\}\Big] + s_{\theta_{\mathrm{B}}}^2\big(\mathcal{C}_2^{22}(1,0)+A_{10}\big)\\
& \times \Big\{\big[\mathcal{C}_0^{11}(1,0) + \mathcal{C}_1^{11}(1,0) + \mathcal{C}_1^{22}(1,0) + \mathcal{C}_2^{22}(1,0)\big]A_{10} + 2A_{10}^2 + g_1^2\omega_{\mathrm{L,1}}^2s_{\theta_{\mathrm{B}}}^2 + \mathcal{C}_0^{11}(1,0)\mathcal{C}_1^{11}(1,0)\\
& + \mathcal{C}_1^{22}(1,0)\mathcal{C}_2^{22}(1,0)\Big\}\bigg] + \big(\mathcal{C}_0^{11}(1,0)+A_{10}\big)\big[\mathcal{C}_1^{12}(1,0)\mathcal{C}_1^{21}(1,0) + \big(\mathcal{C}_1^{11}(1,0)+A_{10}\big)\big(\mathcal{C}_1^{22}(1,0)+A_{10}\big)\big]\\
& \times \big(\mathcal{C}_2^{22}(1,0)+A_{10}\big)^2\Bigg\} \times \Big\{3\mathcal{C}_0^{00}(0,1)\big(\mathcal{C}_0^{00}(1,0)+A_{10}\big) + B_{01}\mathrm{J}_0^0\big(3\mathcal{C}_0^{00}(1,0)-\sqrt{3}\mathcal{T}_0^{00}(0,1)\big)\\
& - 3\big(\mathcal{T}_0^{00}(0,1)+\sqrt{3}A_{10}\big)\mathcal{T}_0^{00}(1,0)\Big\}\Bigg)\rho_0^0(0) \bigg/ \Bigg(\sqrt{6}\bigg\{4g_1^6\omega_{\mathrm{L,1}}^6c_{\theta_{\mathrm{B}}}^6\big(\mathcal{C}_0^{11}(1,0)+A_{10}\big)\\
& + \Big\{g_1^2\omega_{\mathrm{L,1}}^2s_{\theta_{\mathrm{B}}}^2\big(\mathcal{C}_1^{11}(1,0)+A_{10}\big) + \big[\mathcal{C}_1^{12}(1,0)\mathcal{C}_1^{21}(1,0) + \big(\mathcal{C}_1^{11}(1,0)+A_{10}\big)\big(\mathcal{C}_1^{22}(1,0)+A_{10}\big)\big]\\
& \times \big(\mathcal{C}_2^{22}(1,0)+A_{10}\big)\Big\} \times \Big\{g_1^4\omega_{\mathrm{L,1}}^4s_{\theta_{\mathrm{B}}}^4 + g_1^2\omega_{\mathrm{L,1}}^2s_{\theta_{\mathrm{B}}}^2\big[\mathcal{C}_0^{11}(1,0)\mathcal{C}_1^{11}(1,0) + \mathcal{C}_1^{22}(1,0)\mathcal{C}_2^{22}(1,0)\\
& + \big(\mathcal{C}_0^{11}(1,0) + \mathcal{C}_1^{11}(1,0) + \mathcal{C}_1^{22}(1,0) + \mathcal{C}_2^{22}(1,0)\big)A_{10} + 2A_{10}^2\big] + \big(\mathcal{C}_0^{11}(1,0)+A_{10}\big)\\
& \times \big(\mathcal{C}_0^{11}(1,0)+A_{10}\big)\big[\mathcal{C}_1^{12}(1,0)\mathcal{C}_1^{21}(1,0) + \big(\mathcal{C}_1^{11}(1,0)+A_{10}\big)\big(\mathcal{C}_1^{22}(1,0)+A_{10}\big)\big]\big(\mathcal{C}_2^{22}(1,0)+A_{10}\big)\Big\}\\
& + c_{\theta_{\mathrm{B}}}^4\Big\{4g_1^6s_{\theta_{\mathrm{B}}}^2\omega_{\mathrm{L,1}}^6\big(\mathcal{C}_1^{11}(1,0)-\mathcal{C}_0^{11}(1,0)\big) + g_1^4\omega_{\mathrm{L,1}}^4\big(\mathcal{C}_0^{11}(1,0)+A_{10}\big)\Big[9A_{10}^2 + 2\big[4\big(\mathcal{C}_1^{11}(1,0)\\
& + \mathcal{C}_1^{22}(1,0)\big) + \mathcal{C}_2^{22}(1,0)\big]A_{10} + [\mathcal{C}_2^{22}(1,0)]^2 + 4\big([\mathcal{C}_1^{11}(1,0)]^2 + [\mathcal{C}_1^{22}(1,0)]^2 - 2\mathcal{C}_1^{12}(1,0)\mathcal{C}_1^{21}(1,0)\big)\big]\Big]\Big\}\\
& + g_1^6c_{\theta_{\mathrm{B}}}^2\Big\{\omega_{\mathrm{L,1}}^6s_{\theta_{\mathrm{B}}}^4\big(\mathcal{C}_0^{11}(1,0)-4\mathcal{C}_1^{11}(1,0)-3A_{10}\big) + g_1^4s_{\theta_{\mathrm{B}}}^2\omega_{\mathrm{L,1}}^4\Big[3A_{10}^3 - \big(2\mathcal{C}_0^{11}(1,0)+3\mathcal{C}_1^{11}(1,0)\\
& - 10\mathcal{C}_1^{22}(1,0) - 4\mathcal{C}_2^{22}(1,0)\big)A_{10}^2 + \big\{4[\mathcal{C}_1^{22}(1,0)]^2 + 2\big(\mathcal{C}_0^{11}(1,0) + 4\mathcal{C}_1^{11}(1,0)\big)\mathcal{C}_1^{22}(1,0)\\
& + [\mathcal{C}_2^{22}(1,0)]^2 - 4\big(2\mathcal{C}_0^{11}(1,0) + \mathcal{C}_1^{11}(1,0)\big)\mathcal{C}_1^{11}(1,0) + 8\mathcal{C}_1^{12}(1,0)\mathcal{C}_1^{21}(1,0) + 2\big(\mathcal{C}_0^{11}(1,0) + \mathcal{C}_1^{11}(1,0)\\
& + \mathcal{C}_1^{22}(1,0)\big)\mathcal{C}_2^{22}(1,0)\big\}A_{10} + \mathcal{C}_1^{11}(1,0)[\mathcal{C}_2^{22}(1,0)]^2 + 4\mathcal{C}_1^{22}(1,0)\big(\mathcal{C}_1^{12}(1,0)\mathcal{C}_1^{21}(1,0) + \mathcal{C}_1^{11}(1,0)\mathcal{C}_1^{22}(1,0)\big)\\
& + \mathcal{C}_0^{11}(1,0)\big\{-4[\mathcal{C}_1^{11}(1,0)]^2 + 4\mathcal{C}_1^{12}(1,0)\mathcal{C}_1^{21}(1,0) + 2\mathcal{C}_1^{22}(1,0)\mathcal{C}_2^{22}(1,0)\big\}\Big] + g_1^2\omega_{\mathrm{L,1}}^2\big(\mathcal{C}_0^{11}(1,0)+A_{10}\big)\\
& \times \Big[6A_{10}^4 + 2\big\{5\big(\mathcal{C}_1^{11}(1,0) + \mathcal{C}_1^{22}(1,0)\big) + 2\mathcal{C}_2^{22}(1,0)\big\}A_{10}^3 + \big\{5[\mathcal{C}_1^{11}(1,0)]^2 + 16\mathcal{C}_1^{22}(1,0)\mathcal{C}_1^{11}(1,0)\\
& + 5[\mathcal{C}_1^{22}(1,0)]^2 + 2[\mathcal{C}_2^{22}(1,0)]^2 + 6\mathcal{C}_1^{12}(1,0)\mathcal{C}_1^{21}(1,0) + 4\big(\mathcal{C}_1^{11}(1,0) + \mathcal{C}_1^{22}(1,0)\big)\mathcal{C}_2^{22}(1,0)\big\}A_{10}^2\\
& + 2\big\{\big(\mathcal{C}_1^{11}(1,0) + \mathcal{C}_1^{22}(1,0)\big)[\mathcal{C}_2^{22}(1,0)]^2 + \big([\mathcal{C}_1^{11}(1,0)]^2 + [\mathcal{C}_1^{22}(1,0)]^2 - 2\mathcal{C}_1^{12}(1,0)\mathcal{C}_1^{21}(1,0)\big)\mathcal{C}_2^{22}(1,0)\\
& + 4\big(\mathcal{C}_1^{11}(1,0)+\mathcal{C}_1^{22}(1,0)\big) \times \big(\mathcal{C}_1^{12}(1,0)\mathcal{C}_1^{21}(1,0) + \mathcal{C}_1^{11}(1,0)\mathcal{C}_1^{22}(1,0)\big)\big\}A_{10} + \big([\mathcal{C}_1^{11}(1,0)^2 + [\mathcal{C}_1^{22}(1,0)]^2\\
& - 2\mathcal{C}_1^{12}(1,0)\mathcal{C}_1^{21}(1,0)\big)[\mathcal{C}_2^{22}(1,0)]^2 + 4\big(\mathcal{C}_1^{12}(1,0)\mathcal{C}_1^{21}(1,0)+\mathcal{C}_1^{11}(1,0)\mathcal{C}_1^{22}(1,0)\big)^2\big]\Big]\bigg\}\\
& \times \bigg\{\mathcal{C}_0^{02}(1,0)\mathcal{T}_0^{00}(0,1) + \big(\sqrt{3}\mathcal{C}_0^{02}(1,0) - \mathcal{T}_0^{02}(0,1)\big)A_{10} - \mathcal{C}_0^{00}(1,0)\mathcal{T}_0^{02}(0,1)\bigg\}\Bigg),
\end{aligned}
$$

$$(8)$$

$$
\begin{aligned}
\mathrm{Im}\rho_1^1(1) = &-\Bigg(\sqrt{\frac{2}{3}}g_1^2\omega_{\mathrm{L,1}}^2 s_{\theta_{\mathrm{B}}}c_{\theta_{\mathrm{B}}}\mathcal{C}_1^{12}(1,0)\Big[g_1^2\omega_{\mathrm{L,1}}^2\big\{4c_{\theta_{\mathrm{B}}}^2\big(\mathcal{C}_1^{11}(1,0)+\mathcal{C}_1^{22}(1,0)+2A_{10}\big)\\
&+s_{\theta_{\mathrm{B}}}^2\big(-2\mathcal{C}_1^{11}(1,0)+\mathcal{C}_2^{22}(1,0)-A_{10}\big)\big\}+\big(\mathcal{C}_1^{11}(1,0)+\mathcal{C}_1^{22}(1,0)+2A_{10}\big)\big(\mathcal{C}_2^{22}(1,0)+A_{10}\big)^2\Big]\\
&\Big[-3\mathcal{C}_0^{00}(0,1)\big(\mathcal{C}_0^{00}(1,0)+A_{10}\big)+B_{01}\mathrm{J}_0^0\big(\sqrt{3}\mathcal{T}_0^{00}(0,1)-3\mathcal{C}_0^{00}(1,0)\big)+3\big(\mathcal{T}_0^{00}(0,1)+\sqrt{3}A_{10}\big)\mathcal{T}_0^{00}(1,0)\Big]\Bigg)\\
&\times\rho_0^0(0)\Bigg/\Bigg(\Bigg\{\Big[-g_1^2\omega_{\mathrm{L,1}}^2c_{\theta_{\mathrm{B}}}^2\big(2\mathcal{C}_1^{22}(1,0)+\mathcal{C}_2^{22}(1,0)+3A_{10}\big)+\mathcal{C}_1^{12}(1,0)\mathcal{C}_1^{21}(1,0)\big(\mathcal{C}_2^{22}(1,0)+A_{10}\big)\\
&+\big\{g_1^2\omega_{\mathrm{L,1}}^2s_{\theta_{\mathrm{B}}}^2+big(\mathcal{C}_0^{11}(1,0)+A_{10}\big)\big(\mathcal{C}_1^{11}(1,0)+A_{10}\big)\big\}\big\{g_1^2\omega_{\mathrm{L,1}}^2\big(1-3c_{\theta_{\mathrm{B}}}^2\big)\\
&+\big(\mathcal{C}_1^{22}(1,0)+A_{10}\big)\big(\mathcal{C}_2^{22}(1,0)+A_{10}\big)\big\}/\big\{\mathcal{C}_0^{11}(1,0)+A_{10}\big\}\Big]\times\Big[g_1^2\omega_{\mathrm{L,1}}^2\big\{4c_{\theta_{\mathrm{B}}}^2\big(\mathcal{C}_1^{11}(1,0)+\mathcal{C}_1^{22}(1,0)+2A_{10}\big)\\
&+s_{\theta_{\mathrm{B}}}^2\big(-2\mathcal{C}_1^{11}(1,0)+\mathcal{C}_2^{22}(1,0)-A_{10}\big)\big\}+\big(\mathcal{C}_1^{11}(1,0)+\mathcal{C}_1^{22}(1,0)+2A_{10}\big)\times\big(\mathcal{C}_2^{22}(1,0)+A_{10}\big)^2\Big]\\
&+\Big[g_1^2\omega_{\mathrm{L,1}}^2\big(3c_{\theta_{\mathrm{B}}}^2-1\big)-2\mathcal{C}_1^{12}(1,0)\mathcal{C}_1^{21}(1,0)-2\mathcal{C}_1^{11}(1,0)\mathcal{C}_1^{22}(1,0)-\big\{3\big(\mathcal{C}_1^{11}(1,0)+\mathcal{C}_1^{22}(1,0)\big)\\
&+2\mathcal{C}_2^{22}(1,0)\big\}A_{10}-\big(\mathcal{C}_1^{11}(1,0)+\mathcal{C}_1^{22}(1,0)\big)\mathcal{C}_2^{22}(1,0)-4A_{10}^2\Big]\Big[g_1^2\omega_{\mathrm{L,1}}^2c_{\theta_{\mathrm{B}}}^2\big\{\big[2g_1^2\omega_{\mathrm{L,1}}^2\big(1-3c_{\theta_{\mathrm{B}}}^2\big)\\
&-\big(\mathcal{C}_2^{22}(1,0)+A_{10}\big)^2\big\}+\mathcal{C}_1^{12}(1,0)\mathcal{C}_1^{21}(1,0)\times\big\{4g_1^2\omega_{\mathrm{L,1}}^2c_{\theta_{\mathrm{B}}}^2+\big(\mathcal{C}_2^{22}(1,0)+A_{10}\big)^2\big\}\\
&+\big\{g_1^2\omega_{\mathrm{L,1}}^2s_{\theta_{\mathrm{B}}}^2+\big(\mathcal{C}_0^{11}(1,0)+A_{10}\big)\big(\mathcal{C}_1^{11}(1,0)+A_{10}\big)\big\}\big\{g_1^2\omega_{\mathrm{L,1}}^2\big[4c_{\theta_{\mathrm{B}}}^2\big(\mathcal{C}_1^{22}(1,0)+A_{10}\big)\\
&+s_{\theta_{\mathrm{B}}}^2\big(\mathcal{C}_2^{22}(1,0)+A_{10}\big)\big]+\big(\mathcal{C}_1^{22}(1,0)+A_{10}\big)\big(\mathcal{C}_2^{22}(1,0)+A_{10}\big)^2\big\}/\big\{\mathcal{C}_0^{11}(1,0)+A_{10}\big\}\Big]\Bigg\}\\
&\times\Bigg\{\mathcal{C}_0^{02}(1,0)\mathcal{T}_0^{00}(0,1)+A_{10}\big(\sqrt{3}\mathcal{C}_0^{02}(1,0)-\mathcal{T}_0^{02}(0,1)\big)-\mathcal{C}_0^{00}(1,0)\mathcal{T}_0^{02}(0,1)\Bigg\}\Bigg),
\end{aligned}
\tag{9}
$$

where we have defined $s_{\theta_{\mathrm{B}}}\equiv\sin\theta_{\mathrm{B}}$ and $c_{\theta_{\mathrm{B}}}\equiv\cos\theta_{\mathrm{B}}$. In the case at hand, circular SP is generated which is again attributed to the breaking of axial symmetry of the problem. This can be verified from Equations (7), (8) and (9) by setting $s_{\theta_{\mathrm{B}}}=0$ or π, i.e., by making z_{pert} and z_{mag} respectively parallel or anti-parallel, which yields

$$\rho_0^1(1)=\mathrm{Re}\rho_1^1(1)=\mathrm{Im}\rho_1^1(1)=0\,.$$

In other words, restoring the cylindrical symmetry of the problem results in a vanishing circular SP. It can be verified from Equations (7), (8) and (9) that circular SP would be present if θ_{B} is neither zero nor π. In particular, we have verified that, for the special case of $\theta_{\mathrm{B}}=\pi/2$, $\rho_0^1(1)=\mathrm{Im}\rho_1^1(1)=0$ but $\mathrm{Re}\rho_1^1(1)\neq0$.

3.3 Anisotropic Radiation and Oriented Magnetic Field

For completeness, let us also consider the case in which an ensemble of atoms is illuminated by anisotropic radiation in the presence of an oriented magnetic field. We could also allow the atoms to undergo isotropic collisions. The SEE describing this situation are obtained from those in Appendix A by setting all collisional rates with $k\neq k'$ or with $q\neq0$ to zero. Solving for the density matrix elements,

one can verify that

$$\rho_0^1(1)=\mathrm{Re}\rho_1^1=\mathrm{Im}\rho_1^1=0\,.$$

Clearly, the generation of circular SP is not possible in this case despite the breaking of axial symmetry in the problem. This is due to the fact that a weak magnetic field cannot cause the mixing of density matrix elements with different order, k, besides the restriction imposed by selection rules on the possible optical transitions which prevents the mixing between odd- and even-order density matrix elements (see e.g., sects. 7.11 and 10.8 Landi Degl'Innocenti & Landolfi 2004). The later obstacle is not present in the case of anisotropic collisions. That is the reason, in the case of anisotropic collisions, the breaking of cylindrical symmetry leads to the generation of circular SP whereas there is no creation of circular SP if the anisotropy in collisions is replaced by a deterministic weak magnetic field.

4 CONCLUSIONS

We formulated the circularly polarizing effect of anisotropic collisions in the presence of an anisotropic radiation field and/or deterministic magnetic field. In particular, we confirm the possibility of creating atomic circular SP if the density of perturbers is sufficient for anisotropic collisions to be effective. This physical situation can occur in a plasma where charged particles (e.g., protons or electrons) move in a direction different from that photons most frequently are moving in and/or different from that of the magnetic field, in a way that cylindrical symmetry of the problem is broken.

In order to contribute to interpretations of chromospheric Hα line observations of hydrogen (López Ariste et al. 2005; Ramelli et al. 2005), it is important to calculate the relaxation and transfer rates due to anisotropic collisions of hydrogen atoms with electrons. Then, it is necessary to introduce them in a code of resolution of the SEE in order to determine the circular polarization. In addition, in the low corona, it is now well-established that the velocity distributions of the solar wind's electrons, protons and heavy ions are non-thermal, meaning that they are anisotropic and cannot be described by a Maxwellian distribution (e.g., Pilipp et al. 1987 and Pierrard & Lamy 2001). Different models are proposed to represent those distributions, like bi-Maxwellian or kappa distributions (e.g., Maksimovic et al. 1997). Solar wind diagnostics are traditionally based on spectroscopic analysis, which only relies on the Stokes-I measurements. Our results can be used to gain a better understanding of the solar wind physics since the polarization is very sensitive to the anisotropic part of velocity distributions.

Appendix A: SEE

Assuming steady state and utilizing conjugation properties of the density matrix, $\left[\rho_q^k(\alpha_i J_{\alpha_i})\right]^* = (\text{-}1)^q \rho_{\text{-}q}^k(\alpha_i J_{\alpha_i})$, and the radiation field tensor, $\left[J_{q_r}^{k_r}(\nu_{\alpha_i J_{\alpha_i}, j J_{\alpha_j}})\right]^* = (\text{-}1)^{q_r} J_{\text{-}q_r}^{k_r}(\nu_{\alpha_i J_{\alpha_i}, j J_{\alpha_j}})$, and the symmetry properties of the collision rates, given by Equations (3) and (2), the set of coupled SEE can be written as (where $J_{\alpha_i} = 0$ and $J_{\alpha_j} = 1$)[2]:

$$\left(\mathcal{C}_0^{00}(0,1) + B_{01}J_0^0\right)\rho_0^0(0) - \left(\mathcal{T}_0^{00}(0,1) + \sqrt{3}A_{10}\right)\rho_0^0(1) - \mathcal{T}_0^{02}(0,1)\rho_0^2(1) = 0\,, \tag{A.1}$$

$$\left(\mathcal{T}_0^{00}(1,0) + \frac{1}{\sqrt{3}}B_{01}J_0^0\right)\rho_0^0(0) - \left(\mathcal{C}_0^{00}(1,0) + A_{10}\right)\rho_0^0(1) - \mathcal{C}_0^{02}(1,0)\rho_0^2(1) = 0\,, \tag{A.2}$$

$$\sqrt{2}g_1\omega_{\text{L},1}s_{\theta_\text{B}}\text{Im}\rho_1^1(1) - \left(\mathcal{C}_0^{11}(1,0) + A_{10}\right)\rho_0^1(1) = 0\,, \tag{A.3}$$

$$g_1\omega_{\text{L},1}c_{\theta_\text{B}}\text{Im}\rho_1^1(1) - \left(\mathcal{C}_1^{11}(1,0) + A_{10}\right)\text{Re}\rho_1^1(1) + \mathcal{C}_1^{12}(1,0)\text{Im}\rho_1^2(1) = 0\,, \tag{A.4}$$

$$g_1\omega_{\text{L},1}\left(s_{\theta_\text{B}}\text{Im}\rho_1^2(1) + 2c_{\theta_\text{B}}\text{Im}\rho_2^2(1)\right) - \left(\mathcal{C}_2^{22}(1,0) + A_{10}\right)\text{Re}\rho_2^2(1) + \frac{1}{\sqrt{3}}B_{01}\text{Re}J_2^2\rho_0^0(0) = 0\,, \tag{A.5}$$

$$g_1\omega_{\text{L},1}\left(c_{\theta_\text{B}}\text{Im}\rho_1^2(1) + s_{\theta_\text{B}}\text{Im}\rho_2^2(1)\right) + \mathcal{C}_1^{21}(1,0)\text{Im}\rho_1^1(1) - \left(\mathcal{C}_1^{22}(1,0) + A_{10}\right)\text{Re}\rho_1^2(1)$$
$$+ \frac{1}{\sqrt{3}}B_{01}\text{Re}J_1^2\rho_0^0(0) = 0\,, \tag{A.6}$$

$$\sqrt{6}g_1\omega_{\text{L},1}s_{\theta_\text{B}}\text{Im}\rho_1^2(1) + \left(\mathcal{T}_0^{20}(1,0) + \frac{1}{\sqrt{3}}B_{01}J_0^2\right)\rho_0^0(0) - \mathcal{C}_0^{20}(1,0)\rho_0^0(1) - \left(\mathcal{C}_0^{22}(1,0) + A_{10}\right)\rho_0^2(1) = 0\,, \tag{A.7}$$

$$\frac{1}{2}g_1\omega_{\text{L},1}\left(\sqrt{2}s_{\theta_\text{B}}\rho_0^1(1) + 2c_{\theta_\text{B}}\text{Re}\rho_1^1(1)\right) + \left(\mathcal{C}_1^{11}(1,0) + A_{10}\right)\text{Im}\rho_1^1(1) + \mathcal{C}_1^{12}(1,0)\text{Re}\rho_1^2(1) = 0\,, \tag{A.8}$$

$$g_1\omega_{\text{L},1}\left(s_{\theta_\text{B}}\text{Re}\rho_1^2(1) + 2c_{\theta_\text{B}}\text{Re}\rho_2^2(1)\right) + \left(\mathcal{C}_2^{22}(1,0) + A_{10}\right)\text{Im}\rho_2^2(1) + \frac{1}{\sqrt{3}}B_{01}\text{Im}J_2^2\rho_0^0(0) = 0\,, \tag{A.9}$$

$$\frac{1}{2}g_1\omega_{\text{L},1}\left[s_{\theta_\text{B}}\left(\sqrt{6}\rho_0^2(1) + 2\text{Re}\rho_2^2(1)\right) + 2c_{\theta_\text{B}}\text{Re}\rho_1^2(1)\right] + \mathcal{C}_1^{21}(1,0)\text{Re}\rho_1^1(1) + \left(\mathcal{C}_1^{22}(1,0) + A_{10}\right)\text{Im}\rho_1^2(1)$$
$$+ \frac{1}{\sqrt{3}}B_{01}\text{Im}J_1^2\rho_0^0(0) = 0\,, \tag{A.10}$$

where we have defined $\mathcal{C}_q^{kk'}(J_{\alpha_i}, J_{\alpha_j}) \equiv \mathcal{R}_q^{kk'}(J_{\alpha_i} \to J_{\alpha_j}) + \mathcal{R}_q^{kk'}(J_{\alpha_i} \to J_{\alpha_i}) - \mathcal{T}_q^{kk'}(J_{\alpha_i} \leftarrow J_{\alpha_i}) \equiv \mathcal{R}_q^{kk'}(J_{\alpha_i}, J_{\alpha_j}) + \mathcal{R}_q^{kk'}(J_{\alpha_i}) - \mathcal{T}_q^{kk'}(J_{\alpha_i})$ [e.g. $\mathcal{C}_1^{12}(1,0) = \mathcal{R}_1^{12}(1,0) + \mathcal{R}_1^{12}(1) - \mathcal{T}_1^{12}(1)$], $s_{\theta_B} \equiv \sin\theta_B$ and $c_{\theta_B} \equiv \cos\theta_B$. The system of equations above, having a zero determinant, is not closed; consequently, one cannot solve for all density matrix elements. To overcome this issue, the usual practice is to add the trace equation, i.e $\sum_i \sqrt{2J_{\alpha_i}+1}\rho_0^0(J_{\alpha_i}) = N$ with N being the population number, to the system of equations in order to enable the solution for all density matrix elements. However, in the case at hand we are interested only in the orientation terms, $\rho_q^{k=1}$. Therefore, we solve the SEE to obtain $\rho_q^{k=1}$ in terms of the population of the lower level, $\rho_0^0(0)$, which is expected to be non-zero since the lifetime of the lower level is large compared to the upper level. For this purpose, we rely on the algebraic program Mathematica.

References

Bommier, V., & Sahal-Brechot, S. 1978, A&A, 69, 57

del Pino Alemán, T., Trujillo Bueno, J., Stepán, J., & Shchukina, N. 2018, ApJ, 863, 164

Derouich, M. 2007, A&A, 466, 683

Derouich, M., Sahal-Bréchot, S., Barklem, P. S., & O'Mara, B. J. 2003, A&A, 404, 763

Derouich, M., Trujillo Bueno, J., & Manso Sainz, R. 2007, A&A, 472, 269

D'yakonov, M. I., & Perel, V. I. 1978, Sixth Internat. Conf. Atomic phys., Proceedings, Riga, 410, *https://link.springer.com/chapter/10.1007/978-1-4615-9113-9_20*

Hanle, W. 1924, Zeitschrift Fur Physik, 30, 93

Landi Degl'Innocenti, E., & Landolfi, M. 2004, Polarization in Spectral Lines, 307

López Ariste, A., Casini, R., Paletou, F., et al. 2005, ApJ, 621, L145

Maksimovic, M., Pierrard, V., & Lemaire, J. F. 1997, A&A, 324, 725

Manabe, T., Yabuzaki, T., & Ogawa, T. 1979, Phys. Rev. A, 20, 1946

Manabe, T., Yabuzaki, T., & Ogawa, T. 1981, Phys. Rev. Lett., 46, 637

Omont, A. 1977, Progress in Quantum Electronics, 5, 69

Petrashen', A. G., Rebane, V. N., & Rebane, T. K. 1993, Soviet Journal of Experimental and Theoretical Physics, 77, 187

Pierrard, V., & Lamy, H. 2001, Sol. Phys., 216, 47

Pilipp, W. G., Miggenrieder, H., Montgomery, M. D., et al. 1987, J. Geophys. Res., 92, 1075

Ramelli, R., Bianda, M., Trujillo Bueno, J., et al. 2005, in Proc. International Scientific Conference on Chromospheric and Coronal Magnetic Fields (ESA SP-596). Innes D. E., Lagg, A., & Solanki, S. K. (eds), Published on CDROM, 82.1, *http://adsabs.harvard.edu/full/2005ESASP.596E..82R*

Roberto Casini, R., & Manso Sainz, R. 2006, J. Phys. B, 39, 3241

Sahal-Brechot, S. 1977, ApJ, 213, 887

Sahal-Brechot, S., Vogt, E., Thoraval, S., & Diedhiou, I. 1996, A&A, 309, 317

Trujillo Bueno, J. 2001, in Astronomical Society of the Pacific Conference Series, 236, Advanced Solar Polarimetry – Theory, Observation and Instrumentation, ed. M. Sigwarth, 161

Vogt, E., Sahal-Bréchot, S., & Bommier, V. 2001, A&A, 374, 1127